

## Supporting Information

### Metal–Organic Framework-Derived Hollow $\text{Co}_9\text{S}_8$ Nanotube Arrays Coupled with Porous FeCo-P Nanosheets as Efficient Cathode Electrode Material for Hybrid Supercapacitor

Kosar Alitabar, Akbar Mohammadi Zardkhoshoui\* and Saied Saeed Hosseiny Davarani\*

Department of Chemistry, Shahid Beheshti University, G. C., 1983963113, Evin, Tehran, Iran.

Corresponding authors: \*Tel: +98 21 22431661; Fax: +98 21 22431661; E-mail: [ss-hosseiny@sbu.ac.ir](mailto:ss-hosseiny@sbu.ac.ir) (S.S.H. Davarani); and [mohammadi.bahadoran@gmail.com](mailto:mohammadi.bahadoran@gmail.com) (A. Mohammadi Zardkhoshoui)

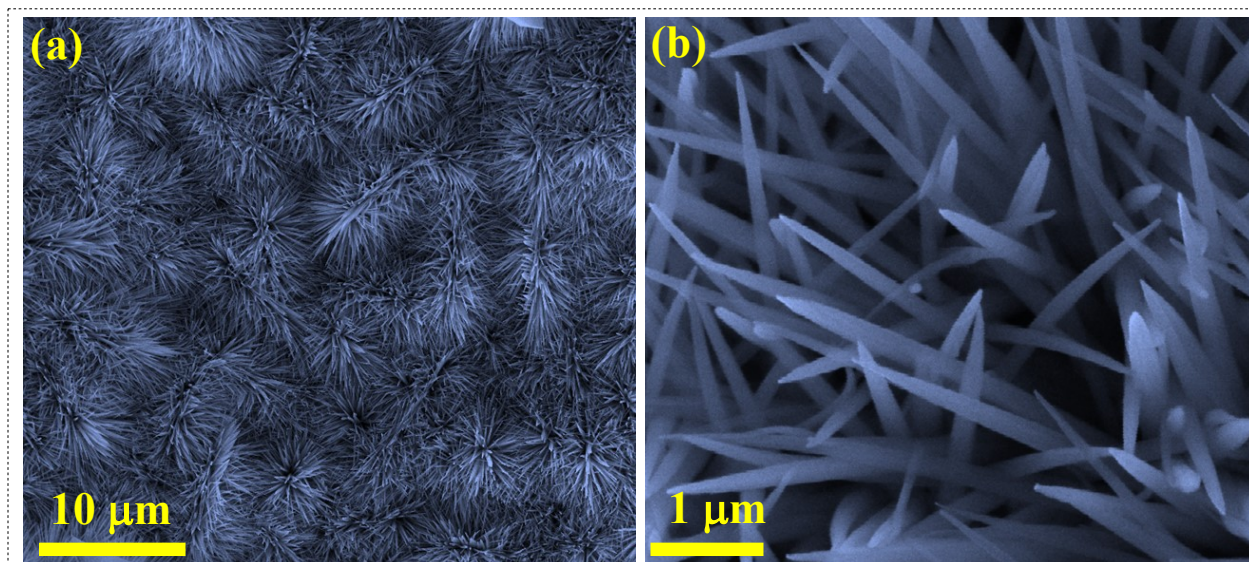


**Fig. S1** (a, b) FE-SEM images of the NF/ $\text{Co}(\text{CO}_3)_{0.5}(\text{OH})$  precursors.

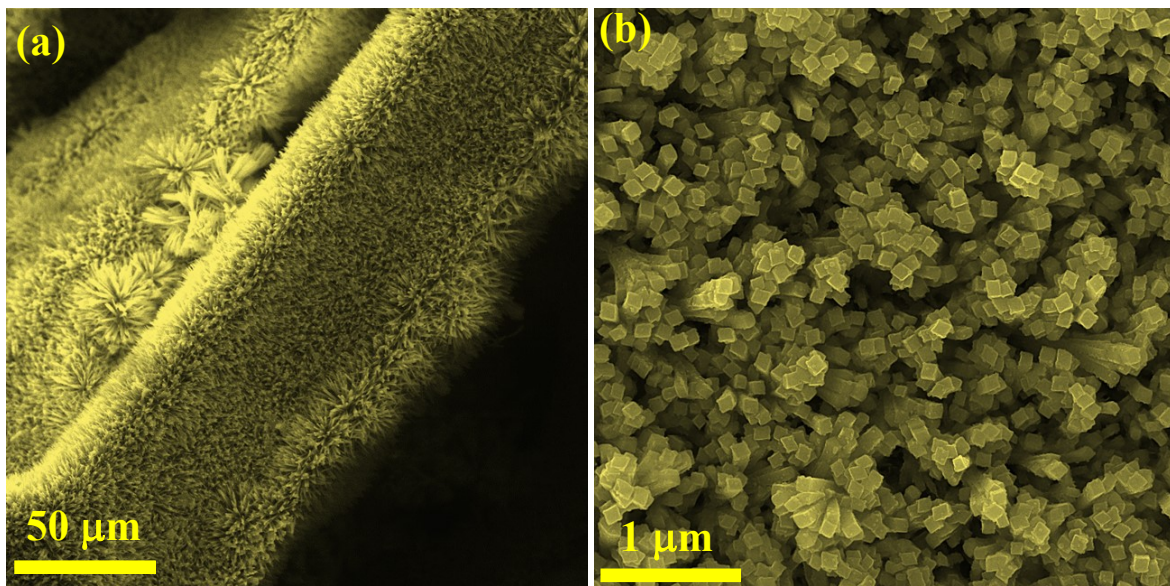


**Fig. S2** (a, b) FE-SEM images of the NF/Co-MOF.

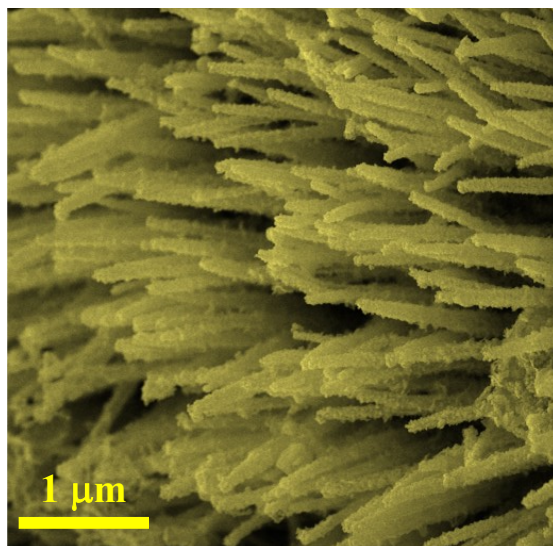


**Fig. S3** FE-SEM image of the NF/CS.

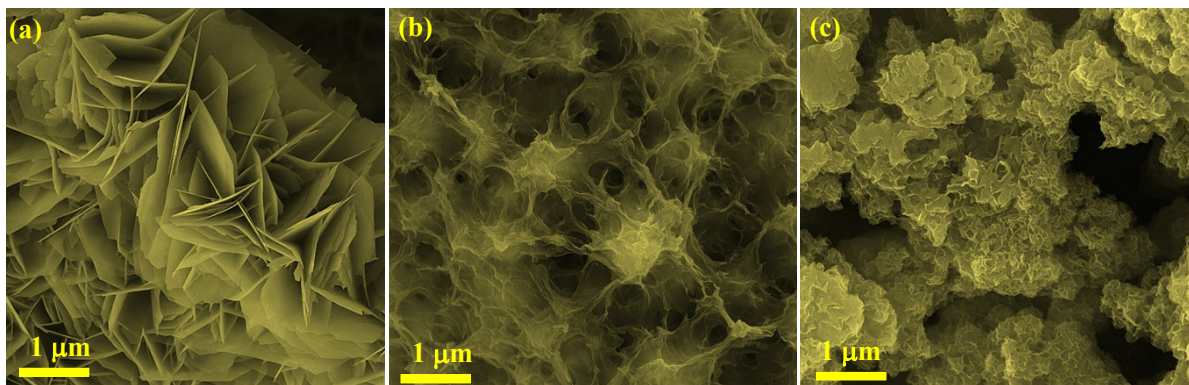


**Fig. S4** (a) FE-SEM image of the NF/FCP20. (b) FE-SEM image of the NF/FCP30. (c) (a) FE-SEM image of the NF/FCP40.

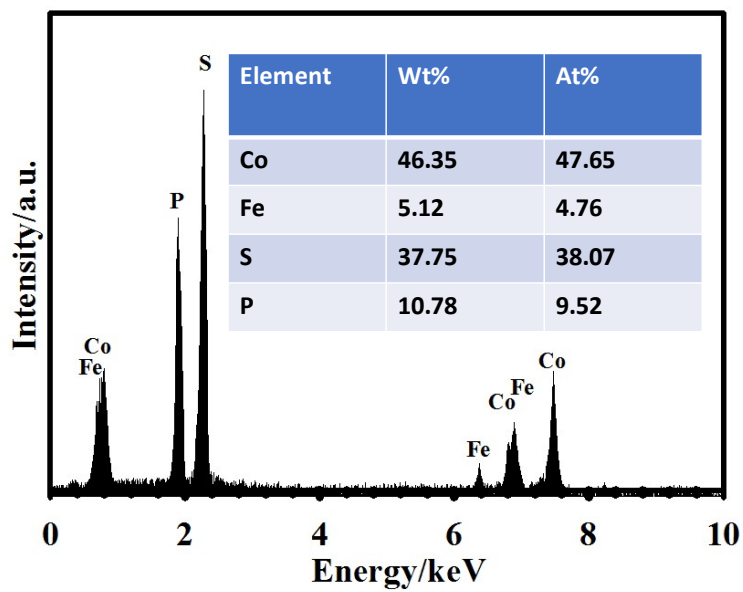


**Fig. S5** EDX pattern of the CS4-FCP30 sample.

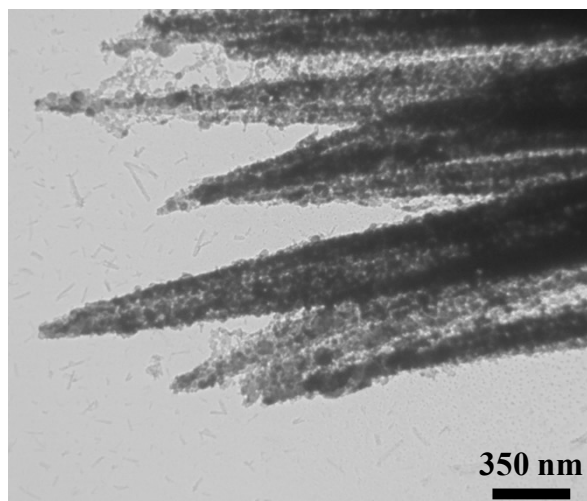


Fig. S6 TEM image of the CS sample.

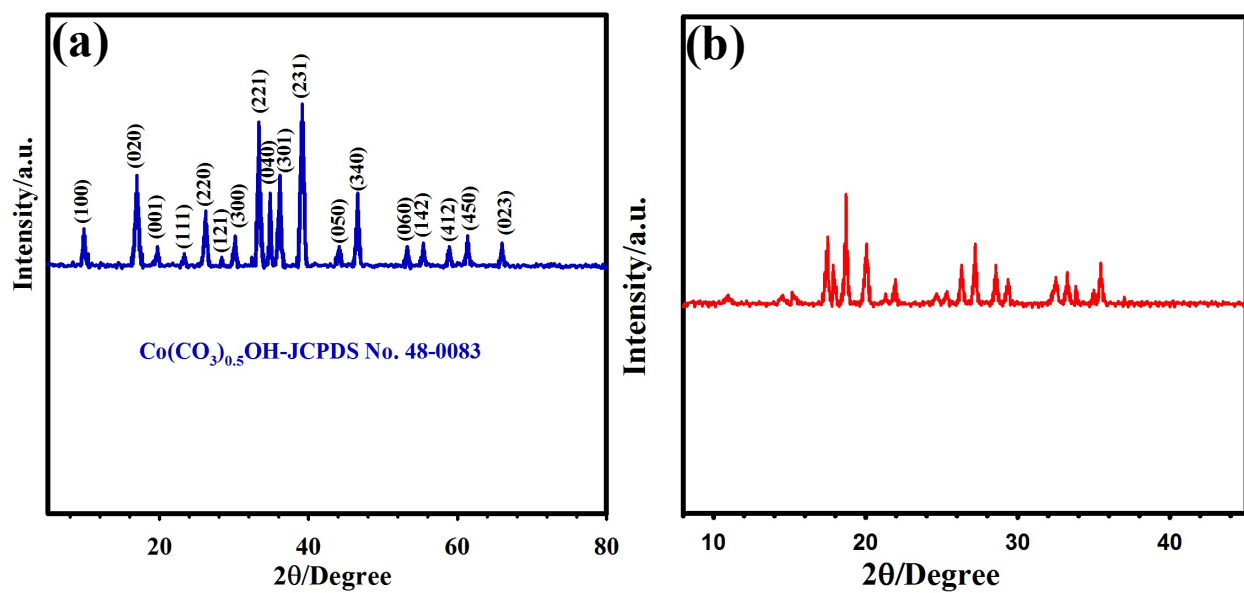
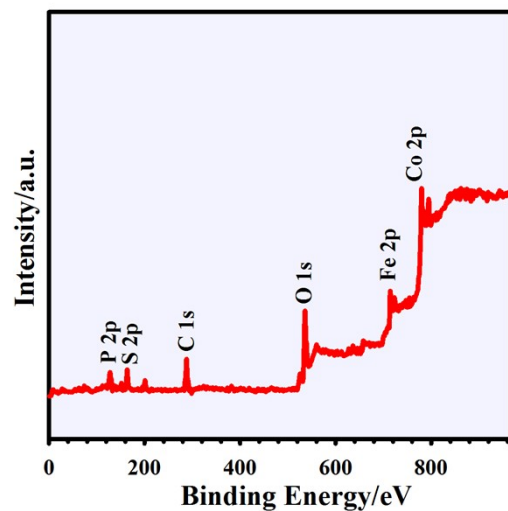
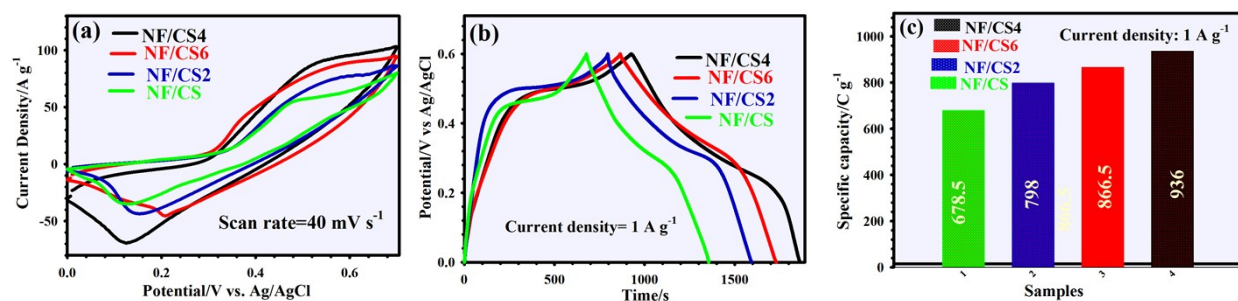


Fig. S7 (a) XRD pattern of the  $\text{Co}(\text{CO}_3)_{0.5}(\text{OH})$ . (b) XRD pattern of the Co-MOF.



**Fig. S8** XPS survey of the CS4-FCP30.



**Fig. S9** (a) CVs of the NF/CS, NF/CS2, NF/CS4, and NF/CS6 electrodes at 40 mV s<sup>-1</sup>. (B) GCD curves of the NF/CS, NF/CS2, NF/CS4, and NF/CS6 electrodes at 1 A g<sup>-1</sup>. (c) Specific capacities of the NF/CS, NF/CS2, NF/CS4, and NF/CS6 electrodes at 1 A g<sup>-1</sup>.

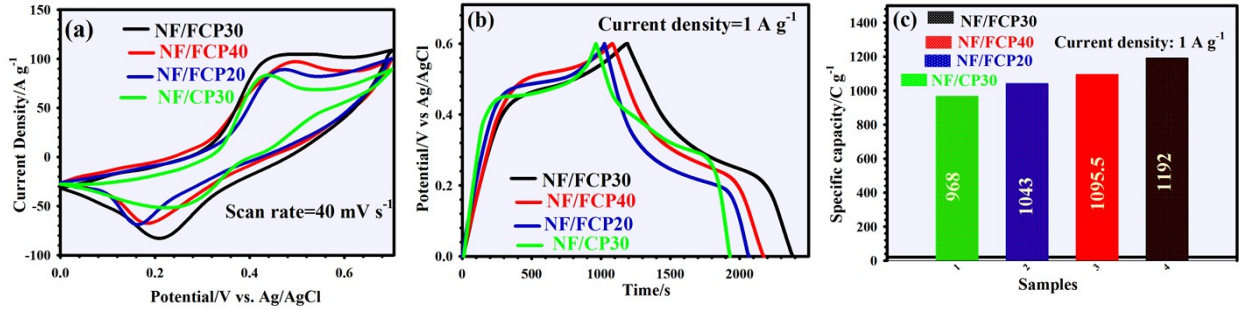


**Fig. S10** (a) CVs of the NF/CP30, NF/FCP20, NF/FCP30, and NF/FCP40 electrodes at  $40 \text{ mV s}^{-1}$ . (B) GCD curves of the NF/CP30, NF/FCP20, NF/FCP30, and NF/FCP40 electrodes at  $1 \text{ A g}^{-1}$ . (c) Specific capacities of the NF/CP30, NF/FCP20, NF/FCP30, and NF/FCP40 electrodes at  $1 \text{ A g}^{-1}$ .

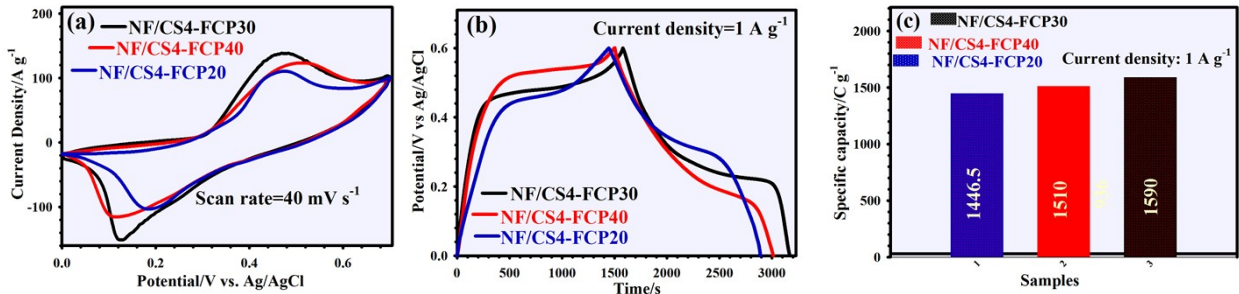


**Fig. S11** (A) CVs of the NF/CS4-FCP20, NF/CS4-FCP30, and NF/CS4-FCP40 electrodes at  $40 \text{ mV s}^{-1}$ . (B) GCD curves of the NF/CS4-FCP20, NF/CS4-FCP30, and NF/CS4-FCP40 electrodes at  $1 \text{ A g}^{-1}$ . (C) Specific capacities of the NF/CS4-FCP20, NF/CS4-FCP30, and NF/CS4-FCP40 electrodes at  $1 \text{ A g}^{-1}$ .

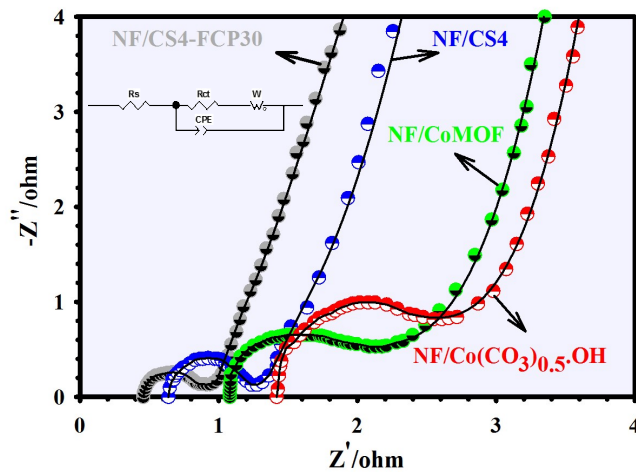


**Fig. S12** Nyquist plots of the NF/Co(CO<sub>3</sub>)<sub>0.5</sub>(OH), NF/Co-MOF, NF/CS4, and NF/CS4-FCP30 electrodes (inset indicate the equivalent circuit model and magnified Nyquist curves).

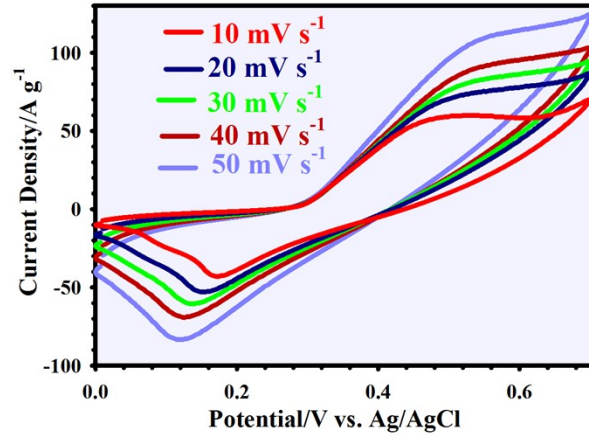


Fig. S13 CV curves of the NF/CS4 electrode at various scan rates from 10 to 50  $\text{mV s}^{-1}$ .

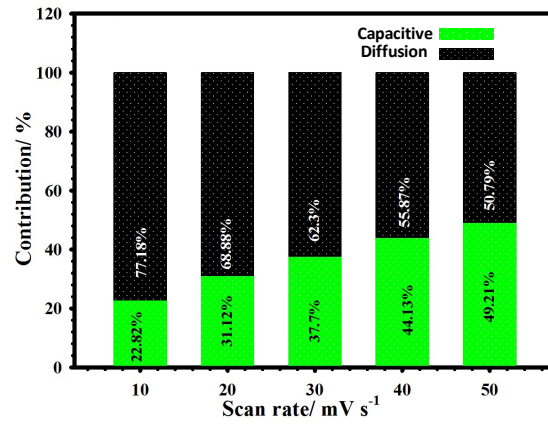


Fig. S14 Relative contribution of the capacitive and diffusion-controlled charge storage at various sweep speeds.

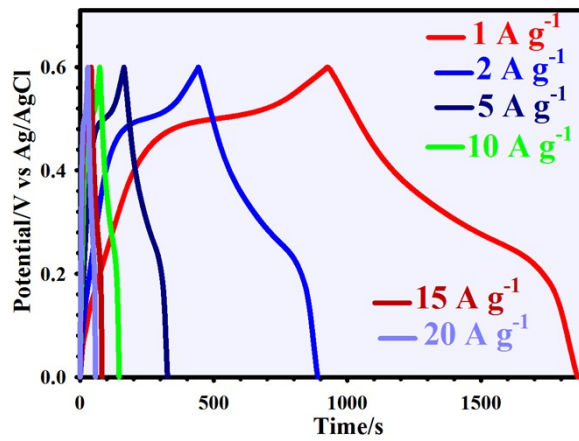


Fig. S15 GCD curves of the NF/CS4 electrode from 1 to 20  $\text{A g}^{-1}$ .

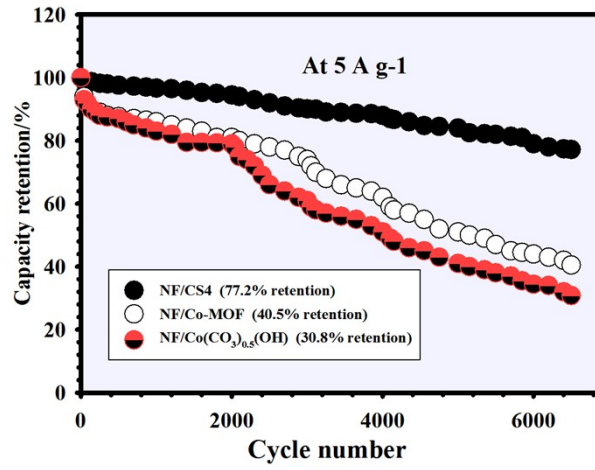


Fig. S16 Durability test of the NF/Co(CO<sub>3</sub>)<sub>0.5</sub>(OH), NF/Co-MOF, and NF/CS4 electrodes

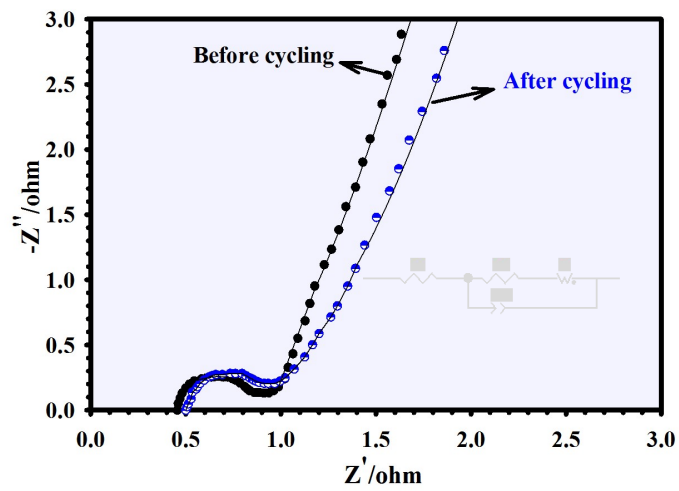


Fig. S17 Nyquist plots of the NF/CS4-FCP30 before and after durability test.



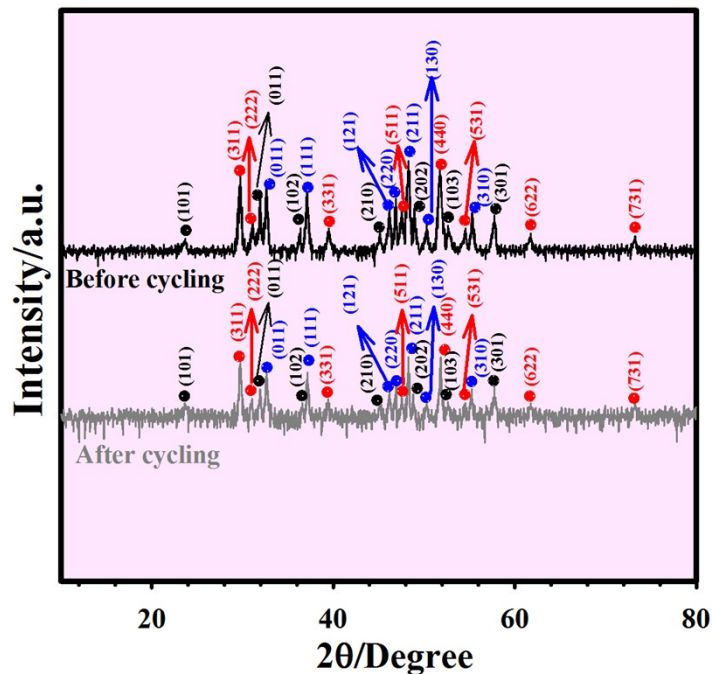


Fig. S18 XRD patterns of the CS4-FCP30 before and after durability test.

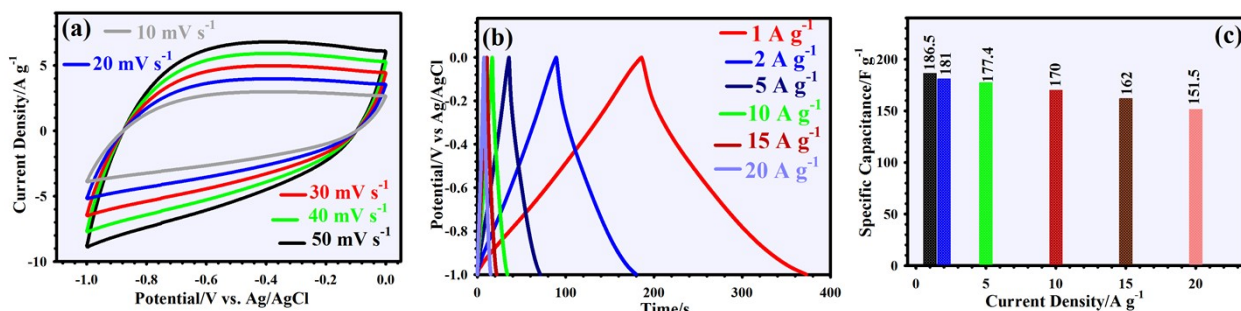


Fig. S19 (a) CV plots of the NF/AC at various scan rates from 10 to 50 mV s<sup>-1</sup>. (b) GCD plots of the NF/AC@ at various current densities from 1 to 20 A g<sup>-1</sup>. (c) Rate capability of the NF/AC electrode.

**Table S1.** Elemental composition of the CS4-FCP30 estimated by ICP-OE.

<b>Element</b>	<b>Wt%</b>	<b>At%</b>
<b>Co</b>	<b>45.35</b>	<b>46.84</b>
<b>Fe</b>	<b>4.88</b>	<b>4.16</b>
<b>S</b>	<b>38.11</b>	<b>39.16</b>
<b>P</b>	<b>11.66</b>	<b>9.84</b>

Based on the weight of Co (45.35 wt%) and S (38.11 wt%) elements, the content of the  $\text{Co}_9\text{S}_8$  in the CS4-FCP30 is calculated as about 78.925 wt%  $[(45.35/10) \times 9 \text{ wt\%} + 38.11 \text{ wt\%}]$  and the content of the FeCo-P in the CS4-FCP30 is calculated as about 21.075 wt%  $(4.88 \text{ wt\%} + 45.35/10 + 11.66 \text{ wt\%})$ .

Composition	Capacity (C/g)	Cycles, retention	Rate capability	ED (Wh kg <sup>-1</sup> )	Reference
NiCoP	761 at 1 A g <sup>-1</sup>	50000, 90.2%	91.1% at 20 A g <sup>-1</sup>	35.6	1
NiCoMn-S-1.5	657.7 at 1 A g <sup>-1</sup>	50000, 90%	51.61% at 50 A g <sup>-1</sup>	36.3	2
Co <sub>9</sub> S <sub>8</sub>	926 at 1 A g <sup>-1</sup>	8000, 86%	67.4% at 15 A g <sup>-1</sup>	25.49	3
Co <sub>3</sub> S <sub>4</sub> /g-C <sub>3</sub> N <sub>4</sub> -10	415 at 0.5 A g <sup>-1</sup>	5000, 75.6%	54.5% at 10 A g <sup>-1</sup>	37.7	4
NiCoMn-S	661 at 1 A g <sup>-1</sup>	1000, 86.45%	66.56% at 50 A g <sup>-1</sup>	42.1	5
Ni <sub>2</sub> P/NiCoP	741.3 at 1 A g <sup>-1</sup>	30000, 89.2%	75.5% at 50 A g <sup>-1</sup>	44.5	6
Ni-Co-P/POx/C	583 at 1 A g <sup>-1</sup>	5000, 77.3%	62.7% at 30 A g <sup>-1</sup>	37.59	7
NF/CS4-FCP30	1590 at 1 A g <sup>-1</sup>	6500, 92.8 (3 E)	73.3% at 20A g <sup>-1</sup>	66.6	This work

**Table S2.** Comparison of the performance of the NF/CS4-FCP30 with other previously reported materials.

## References

- 1 M. Gao, W.-K. Wang, X. Zhang, J. Jiang and H.-Q. Yu, *J. Phys. Chem. C* 2018, **122**, 25174–25182.
- 2 J. Zhang, C. Li, M. Fan, T. Ma, H. Chen and H. Wang, *Appl. Surf. Sci.* 2021, **565**, 150482.
- 3 J. Li, Q. Li, J. Sun, Y. Ling, K. Tao and L. Han, *Inorg. Chem.* 2020, **59**, 11174–11183.
- 4 W. Li, Y. Li, C. Yang, Q. Ma, K. Tao and L. Han, *Dalton Trans* 2020, **49**, 14017-14029.
- 5 J. Cao, Y. Hu, Y. Zhu, H. Cao, M. Fan, C. Huang, K. Shu, M. He, H. C. Chen, *Chem. Eng. J* 2021, **405**, 126928.

6 Z. Li, K. Ma, F. Guo, C. Ji, H. Mi, P. Qiu and H. Pang, *Mater. Lett.* 2021, **288**, 129319.

7 X. Zhang, J. Wang, Y. Sui, F. Wei, J. Qi, Q. Meng, Y. He and D. Zhuang, *ACS Appl. Nano Mater.* 2020, **3**, 11945–11954.